NOAA Collaborative Science, Technology, and Applied Research (CSTAR) Final Report

Ensemble Subsetting within Optimized Ensembles to Improve Probabilistic Prediction of Severe Convection

Award NA17NWS4680003

Texas Tech University
PIs Brian Ancell and Christopher Weiss

7/1/2017 – 6/30/2021

1. Overview and Statement of Primary Goals

The primary goal of this project has been to develop convective-scale ensemble sensitivity tools to improve probabilistic forecasts of severe convection and its individual hazards. Ensemble sensitivity reveals dynamical relationships between a chosen forecast response function (e.g. updraft helicity at 36-hr forecast time) and the atmospheric state earlier in the forecast window (e.g. 500-hPa geopotential height at 6-hr forecast time). While ensemble sensitivity has been successfully applied at synoptic scales with more linear ensemble perturbation evolution, a thorough examination of convective-scale ensemble sensitivity at TTU has revealed it is just as useful in highlighting the flow features relevant to forecasts of convection. In turn, a formal evaluation of real-time, convective-scale ensemble sensitivity fields was conducted by Texas Tech University (TTU) researchers at the 2016 Hazardous Weather Testbed (HWT) Spring Forecast Experiment (SFE), which showed consistent signals in the sensitivities of convection responses such as updraft helicity, high winds, and simulated reflectivity. These results strongly motivated the use of sensitivity fields to identify the ensemble members early in the forecast window that are most skillful, potentially producing beneficial adjustments to probabilistic forecasts of severe events well before subsequent ensemble forecast initializations – developing such a subsetting technique was the main objective of this work. More generally, applying ensemble sensitivity analysis (ESA) itself to short temporal and spatial scales to identify near-storm controls on convection characteristics like rotation was another primary objective of this work with the ultimate goal of applying such knowledge to Warn on Forecast System (WoFS) applications in the future.

While developing the ensemble sensitivity-based subsetting technique and storm-scale ESA was the main focus of this project, other objectives were involved with this research. An observing system simulation experimental (OSSE) framework has been created at TTU and experiments were conducted to understand how targeted observations within a convection-allowing ensemble data assimilation system may improve probabilistic forecasts of severe convection. Incorporating new forecast products associated with this work into the AWIPS2 system for operational use at the National Weather Service was also a key objective.

2. Research Achievements

A. Ensemble Sensitivity-Based Subsetting for Day 1/Day 2 Forecasts of Convection

Determining whether adjusting an ensemble of forecasts based on choosing a subset of members with the smallest errors in sensitive regions for 12-48hr forecasts of severe convection was a major goal of this project. This capability was demonstrated at synoptic scales for forecasts of midlatitude cyclones by PI Ancell and applying the technique to convection was performed here through several cases of strongly and weakly forced scenarios from the period of April-May 2016. Here this evaluation focused on the magnitude and coverage of different hazards, namely storm rotation (through updraft helicity) or reflectivity valid over 6-hr forecast periods, which were used as the response functions that drove the sensitivity calculations. This effort was conducted through three phases to understand the value of this technique both fundamentally and in a more operational, real-world framework:

Idealized Experiments – These experiments used an ensemble member as truth for choosing ensemble subsets with the smallest early forecast errors in sensitive regions and performed verification against that same member. This allowed direct verification of the response function (e.g. updraft helicity) for which sensitivity was calculated and used for ensemble subsetting. In turn, these experiments demonstrate the fundamental capability of the ensemble subsetting technique with the only obstacle being nonlinearity involved with the sensitivity field itself (i.e. no model physics error, analysis error, or verification issues).

Semi-Idealized Experiments – These experiments also used an ensemble member as truth but involved simulated storm reports generated from the updraft helicity fields in the truth member. This allowed for verification in the same way as the practical experiment which must be verified against actual storm reports. This fostered an understanding of whether the verification required in real-world experiments suffers from the verification technique itself (still without model or analysis error), thereby masking the potential of the ensemble subsetting technique.

Practical Experiments – These experiments use actual analyses as truth for the ensemble subsetting procedure and verify against real storm reports (through Storm Prediction Center practically perfect probabilities). Above and beyond the issues involved with verification against storm reports (which are not directly related to the

sensitivity response functions that must be used), these experiments possess the added complexities of model physics error, analysis error, and the quality of the ensemble in the first place. These experiments are meant to reveal the degree of improvement of the ensemble subsetting technique within more idealized experiments in an operational, real-world framework.

A large number of experimental configurations were used and involved different subset sizes and sets of sensitivity variables (e.g. upper-air only, or near-surface only), and subsetting was performed at 6-hr forecast time.

The idealized experiments showed strong fundamental capability of the ensemble subsetting technique. Figure 1 shows the frequency of all subset configurations tested for different RMSE error reduction against 2-5km updraft helicity values (left panel), as well as the frequency of cases for which each subset produced an improvement (right panel). Nearly all experimental configurations produced error reductions, indicating a strong fundamental capability of the subsetting technique to improve forecasts of updraft helicity. Figure 2 shows the dependence of success on the subset size and shows improvement down to about 15-20 ensemble members at which point smaller subsets reveal diminishing benefits. In turn, about half to just under half of the ensemble is optimal collectively over all configurations tested. Lower atmospheric sensitivity variables produced the most substantial forecast improvements (not shown) within the idealized experiments.

The semi-idealized experiments, which used simulated storm reports from model forecast updraft helicity fields and fractions skill scores (FSS) and reliability as verification metrics, show more modest improvements than the idealized experiments. Figure 3 shows that the subset configurations that improve both metrics are in the minority (upper left quadrant of all panels), and that these improvements are relatively small. Interestingly, since the only difference in these experiments relative to the idealized ones is the use of FSS and reliability against simulated storm reports, these results suggest verifying against storm reports and associated practically perfect probabilities through FSS and reliability is unable to show the fundamental capability of the subsetting technique demonstrated in the idealized simulations. The practical experiments, which further include the effects of analysis error, model error, ensemble quality, and the use of verification against observations not directly diagnosed by the response function provided additional slight degradations beyond the semi-idealized experiments. However, while most

configurations in the practical experiments did not show improvements relative to the full ensemble for both FSS and reliability, a number of subset configurations provided improvements on average. Figure 4 shows these results - the experiments falling into the upper left portion of each panel show improvements in both metrics. When simulated reflectivity is used both for the sensitivity calculations and subsetting (Figure 5), substantially more subsetting configurations produce improvements. This further suggests the use of updraft helicity within subsetting experiments is a major obstacle to realizing the potential of the technique, and when using more easily observed response functions the subsetting technique can be successful in a real-world framework. Future efforts will focus on this difficulty, and will attempt to discern whether other verification techniques or convection-related response functions that are more easily observed (e.g. simulated reflectivity, or precipitation) must be employed in subsetting generally. Further, the dependence of subetting success on flow regime, storm mode, ensemble spread, and response function spread will also be examined with the optimal subsetting configurations found through the work here. More detailed results on the subsetting experiments performed in this project can be found in Coleman and Ancell (2020).

B. Storm-Scale ESA

A goal of the funded work was to establish how Ensemble Sensitivity Analysis (ESA), a tool traditionally applied to synoptic scales of motion, can be used on smaller spatiotemporal scales to glean information about the inherent predictability of severe storm hazards. ESA uses postprocessing of ensemble output to develop a linear relationship between a response metric of interest (e.g., low-level vertical vorticity) and an upstream state variable that is suspected to have influence on that response.

For this project, an ensemble of 50 high-resolution (250 m horizontal grid spacing; vertical grid spacing stretched from 50-250 m) supercells was simulated using Cloud Model Version 1 (CM1). The base state is based on the 24 May 2011 El Reno, Oklahoma tornadic supercell event. In an effort to limit the low-level environmental influence on storm evolution (and, thereby, isolate storm-scale controls), perturbations were only made to the control-member base state above 850 mb, with magnitudes within a typical amount of measurement error. With this method, a reasonable amount of spread in the storm-scale thermodynamics and kinematics

(Figure 6) and resulting tornado-like vortex (TLV) frequency and intensity (Figure 7) was achieved.

Conclusions were made regarding a number of hypotheses using ESA on this idealized ensemble. The response variables are generally positively sensitive to density potential temperature with the rear flank outflow (RFO; Figure 8), consistent with the lessened vertical accelerations (and, therefore, stretching) one would expect as cold RFO air is ingested into the primary updraft of the storm. For many of the responses, the magnitude of low-level vertical vorticity did not linearly covary with RFO temperature; rather, this temperature only needed to exceed a certain threshold value to allow for TLV development. Kinematically, it was found that divergence near the surface to the south of the mesocyclone is important for TLV formation, by forcing convergence of warm environmental air to the north, near the incipient TLV (Figure 9).

In the forward flank of the supercell, all response variables are positively sensitive to density potential temperature in the forward-flank cold pool, specifically behind the cold pool head, roughly 2-4 km west of the forward-flank boundary (FFB; Figure 10), supporting the notion that an ideal middle ground in forward flank outflow temperature exists, whereby baroclinic vorticity can be generated along the leading density gradient, but the air still retains enough positive buoyancy to freely ascend in the updraft and amplify baroclinic (and any environmental barotropic) vorticity. It is important to note that no such significant sensitivity is analyzed along the leading edge of the cold pool, where, based on theory, relevant baroclinic vorticity might be expected to be maximized.

Finally, all response variables appear to be sensitive to the lateral position of the forward-flank boundary in a storm-relative sense, where members producing the strongest vertical vorticity contain a FFB that is located father eastward of the low-level mesocyclone (Figure 11). This association is particularly important within five minutes of TLV formation, and within 5-10 km of the mesocyclone.

Overall, we have shown ESA to be an effective tool when used to identify storm-scale characteristics in supercell thunderstorms that are associated with TLV production and magnitude on short time and spatial scales. While our results identify potential storm-scale controls on supercell tornadogenesis, more work needs to be done using ESA on different types of supercells, especially those that form in more marginal environments. That said, we believe

these types of findings may ultimately provide guidance in the field for targeted observations of supercells to improve storm-scale forecasts.

C. Ensemble Sensitivity-Based Observation Targeting

One of our research initiatives involved the application of ESA for the purposes of hypothetical sensitivity-based observation targeting. For this study, we chose four episodes of severe thunderstorms in the southeastern United States (22 Apr 2017, 30 Apr 2017, 23 Feb 2019, 14 Mar 2019). For each case, observation targeting fields (a combination of the ensemble sensitivity and the variance in the upstream state) were generated to determine where forecasts of 1-6 km AGL updraft helicity was sensitive to low-level thermodynamics.

In the 22 Apr 2017 case (Figure 12), robust targeting regions for 2-m temperature and dewpoint appear as much as eight hours prior to the 2200 UTC response. The targets are a mix of signals related to antecedent convection and the preconvective environment for storms that develop in the afternoon. Overall, the pattern of ESA-identified targets is more coherent for state variables at 850 mb versus the surface, suggesting that near-surface sampling was less important for forecast error variance reduction in this particular case.

The 30 Apr 2017 case (Figure 13) featured a robust quasi-linear convective system (QLCS) that propagated through eastern Mississippi and western Alabama through the early afternoon hours. Unlike the 22 April case, the majority of ESA-based targets at the surface were well behind the convective line at all forecast times, undoubtedly a signal of the importance of observations of the system-generated cold pool. At 850 mb, some targets did exist in the inflow sector across Alabama and near the back side of the QLCS.

The 23 Feb 2019 case (Figure 14) exhibited a similar layout of targets as 30 Apr 2017. Near-surface targets were spatiotemporally incoherent for the most part in the inflow region across Alabama and Georgia; robust targets were largely restricted to areas behind the developing convection in northwestern Mississippi. The 850-mb targeting fields were scattered in the inflow sector, and originated from the Gulf of Mexico.

The final case, 14 Mar 2019 (Figure 15), does present scattered preconvective targets for 2-m temperature by 1800 UTC (3 hours prior to the response), but no such signal was evident for 2-m dewpoint. Similar to the two preceding cases, the bulk of the identified sensitivity for surface variables was behind the convective line.

Overall, ESA-based observation targeting methods reveal relatively narrow spatiotemporal windows for effective targeting in the preconvective environment when considering near-surface variables. A companion study (not shown) considered the impact of assimilating fixed-site non-routine observations across portions of the inflow region and, consistent with the results presented here, identified weak impact on the reduction of forecast error variance. In contrast, target areas were consistently robust within the convectively generated cold pool, highlighting the role of downdraft processes in developing and sustaining storm-scale rotation for, particularly, the quasi-linear convective modes studied. Target regions were overall more coherent for state variables at 850 mb versus at 2 m AGL.

D. Integration of Forecast Products into AWIPS2

Integrating probabilistic forecast products from the TTU real-time ensemble used in this project was a goal toward increasing forecaster familiarity with the quantities that accompany ESA. In this way, a foundation could be built through a more familiar NWS forecaster framework to begin the creation of an optimized ensemble sensitivity-based subsetting tool. TTU researchers worked primarily with Lubbock WFO personnel (Mark Conder and John Holsenbeck) to appropriate configure AWIPS2 files, settings, and parameters, and tested different AWIPS2 configurations that allowed ingestion of forecast fields originally produced within the TTU system. This effort produced basic progress in that a framework was established to ingest brand new variables (appropriately configuring the system to ingest new variables from scratch was a major challenge). While a suite of ingested ensemble products was not finalized during this project, the ability to create these fields in AWIPS2 was achieved and will be built upon in future work.

3. Synergistic Activities Performed with NOAA

The following activity was conducted in direct collaboration with NOAA/NWS personnel during the project:

- SPC (Israel Jirak) to evaluate the TTU sensitivity-based subsetting forecast product at the 2018 HWT Spring Forecast Experiment.
- Lubbock, TX forecast office (Mark Conder and John Holsenbeck) toward integration of TTU forecast products into AWIPS2.
- Norman, OK forecast office (Todd Lindley) to expand the RFTI fire weather product.

- SPC (Israel Jirak) and NSSL (Adam Clark, Brett Roberts) to conduct a larger evaluation of the TTU sensitivity-based subsetting forecast product at the 2019 HWT Spring Forecast Experiment with integration into the NOAA CLUE system.
- Discussions at both the NWS SOOConWest meeting in Amarillo, TX and the NWS MIC meeting in Lubbock, TX about the development and evaluation at individual forecast offices of the ensemble sensitivity-based subsetting technique developed during this project.
- Evaluation of the ensemble sensitivity-based subsetting procedure across multiple platforms at the 2020 HWT Spring Forecast Experiment.
- Participation in the SOOConWest Meeting on Feb. 10, 2020, in order to provide an update on the sensitivity-based subsetting technique toward testing of an operational product at NWS WFOs.
- Discussion with various NWS personnel (e.g. Chad Gravelle, Operations Proving Ground) toward performing real-time testing of the subsetting technique at different WFOs.

4. Dissemination of Results and Graduate Student Involvement

Publications:

1) Hill, A.J., 2019: **Demonstration of Ensemble Sensitivity-based Targeted Observing for Convective-Scale Applications: Perfect-model Experiments**. Ph.D. Dissertation, Texas Tech University, 138 pages.

2) Coleman, A.A., 2019: **Convective-scale Ensemble Subsetting with Ensemble Sensitivity Analysis**. M.S. Thesis, Texas Tech University, 109 pages.

3) Coleman, A.A. and B.C. Ancell, 2020: **Towards the Improvement of High-Impact Probabilistic Forecasts with a Sensitivity-based Convective-scale Ensemble Subsetting Technique**. *Monthly Weather Review*, Vol. 148, pages 4995-5014.

4) Hill, A.J., C.C. Weiss, and B.C. Ancell, 2020: **Factors Influencing Ensemble Sensitivity-based Targeted Observing Predictions at Convection-allowing Resolutions**. *Monthly Weather Review*, Vol. 148, pages 4497-5517.

5) Hill, A. J., C. C. Weiss, and D. Dowell, 2021**: Influence of a Portable Near Surface Observing Network on Experimental Ensemble Forecasts of Deep Convection During VORTEX-SE**. *Weather and Forecasting*, Vol. 36, pages 1141-1167.

Presentations:

1) "**The Nature and Variability of Ensemble Sensitivity Fields that Diagnose Severe Convection**", Brian C. Ancell, American Geophysical Union Fall Meeting, New Orleans, LA, December 13, 2017.

2) "**Ensemble Sensitivity Analysis Based Observation Targeting for Mesoscale Convection Forecasts and Factors Influencing Observation-Impact Prediction**", Aaron J. Hill, C.C. Weiss, and B.C. Ancell, American Geophysical Union Fall Meeting, New Orleans, LA, December 13, 2017.

3) **"Ensemble-Sensitivity Analysis-Based Observation Targeting Experiments for Mesoscale Convection Forecasts and Factors Influencing Observation-Impact Prediction"**, Aaron J. Hill, C.C. Weiss, and B.C. Ancell, 22nd Conference on Integrated

Observing and Assimilation Systems for the Atmosphere, Oceans, and Land Surface (IOAS-AOLS), AMS Annual Meeting, Austin, TX, January 7-11, 2018.
4) **"Determining the Impact of Assimilating Satellite Radiance Data for Forecasts within a Mesoscale Ensemble Kalman Filter"**, Jonathan Madden and B.C. Ancell, 22nd Conference on Integrated Observing and Assimilation Systems for the Atmosphere, Oceans, and Land Surface (IOAS-AOLS), AMS Annual Meeting, Austin, TX, January 7-11, 2018.
5) **"The Nature and Variability of Ensemble Sensitivity Fields that Diagnose Severe Convection"**, Brian C. Ancell, 22nd Conference on Integrated Observing and Assimilation Systems for the Atmosphere, Oceans, and Land Surface (IOAS-AOLS), AMS Annual Meeting, Austin, TX, January 7-11, 2018.
6) **"Ensemble Sensitivity Analysis of Controls on Storm-Scale Vertical Vorticity for Two Southeastern U.S. Tornado Events"**, Christopher C. Weiss, D.C. Dowell, A.J. Hill, and N. Yussouf, 22nd Conference on Integrated Observing and Assimilation Systems for the Atmosphere, Oceans, and Land Surface (IOAS-AOLS), AMS Annual Meeting, Austin, TX, January 7-11, 2018.
7) **"The Nature and Variability of Ensemble Sensitivity Fields that Diagnose Severe Convection"**, Brian C. Ancell, International Symposium on Data Assimilation 2018, Munich, Germany, March 5-9, 2018.
8) "**Sensitivity-Based Ensemble Subsetting at Convective Scales**", A. Coleman and B.C. Ancell, 3rd Annual Texas Weather Conference, Arlington, TX, Sept. 22, 2018.
9) **"Towards Improving Forecasts of Severe Convection along the Dryline Through Targeted Observing with Ensemble Sensitivity Analysis"**, A.J. Hill, C.C. Weiss, and B.C. Ancell, 29th Conference on Severe Local Storms (American Meteorological Society), Stowe, VT, October 26, 2018.
10) **"Convective-Scale Ensemble Subsetting with Ensemble Sensitivity Analysis"**, A. Coleman and B.C. Ancell, 29th Conference on Severe Local Storms (American Meteorological Society), Stowe, VT, October 23, 2018.
11) **"Ensemble Sensitivity-Based Subsetting Overview and Evaluation Activities at the 2018 NOAA HWT"**, B.C. Ancell, A. Coleman, A.J. Hill, and C.C. Weiss, 29th Conference on Severe Local Storms (American Meteorological Society), Stowe, VT, October 22, 2018.
12) **"Preliminary Results from the 2018 National Robotics Initiative Field Project"**, C.C. Weiss, A.L. Houston, E.W. Frew, B. Argrow, A.L. Hutson, and A. Schueth, 29th Conference on Severe Local Storms (American Meteorological Society), Stowe, VT, October 22, 2018.
13) **"The Relationship between RFD Thermodynamic Deficit and RFGF Vertical Structure in High-resolution Simulated Supercells"**, A.L. Hutson, C.C. Weiss, D.C. Dowell, and G.H. Bryan, 29th Conference on Severe Local Storms (American Meteorological Society), Stowe, VT, October 22, 2018.
14) **"Ensemble Sensitivity-Based Subsetting Overview and Evaluation Activities at the 2018 NOAA HWT"**, B.C. Ancell, A. Coleman, A.J. Hill, And C.C. Weiss, American Geophysical Union Annual Meeting, Washington D.C., December 12, 2018.
15) "**Ensemble Sensitivity-Based Subsetting Overview and Evaluation Activities at the 2018 HWT**", B. Ancell, A. Coleman, and A. Hill, 23rd Conference on Integrated Observing and Assimilation Systems for the Atmosphere, Oceans, and Land Surface (IOAS-AOLS), Phoenix, AZ, January 8, 2019.
16) "**Ensemble Sensitivity-Based Subsetting at Convective Scales: Objective Verification**

and Optimization", A. Coleman and B. Ancell, 23rd Conference on Integrated Observing and Assimilation Systems for the Atmosphere, Oceans, and Land Surface (IOAS-AOLS), Phoenix, AZ, January 10, 2019.
17) "**Insights into Mesoscale and Storm-Scale Predictability Gained through Ensemble Sensitivity Analysis**", C. Weiss, D. Dowell, N. Yussouf, and A. Hill, 23rd Conference on Integrated Observing and Assimilation Systems for the Atmosphere, Oceans, and Land Surface (IOAS-AOLS), Phoenix, AZ, January 10, 2019.
18) "**Using Ensemble Sensitivity Analysis to Identify Storm-scale Characteristics Associated with Tornadic Potential in High-resolution Idealized Supercells**", A.L. Hutson, C.C. Weiss, and D.C. Dowell, 23rd Conference on Integrated Observing and Assimilation Systems for the Atmosphere, Oceans, and Land Surface (IOAS-AOLS), Phoenix, AZ, January 10, 2019.
19) "**Ensemble Sensitivity-Based Subsetting Overview and Evaluation Activities at the 2018 HWT**", B. Ancell, A. Coleman, and A. Hill, European Geosciences Union Annual Meeting, Vienna, Austria, April 12, 2019.
20) "**The Use of Ensemble Sensitivity to Improve Probabilistic Forecasts of High-Impact Events**", B. Ancell and A. Coleman, Air Force Weather Agency Seminar Series, Omaha, NE, July 9, 2019.
21) "**Sensitivity-Based Ensemble Subsetting at Convective Scales**", A. Coleman and B. Ancell, 18th Conference on Mesoscale Processes, Savannah, GA, July 29, 2019.
22) "**The Use of Ensemble Sensitivity to Improve Probabilistic Forecasts of High-Impact Events",** B. Ancell and A. Coleman, NWS SOOConWest Workshop, Amarillo, TX, Aug. 21, 2019.
23) "**Developing an Operational Sensitivity-Based Forecast Tool to Improve Probabilistic High-Impact Forecasts**", B. Ancell and A. Coleman, NWS MIC Workshop, Lubbock, TX, Sept. 17, 2019.
24) "**The Nature and Variability of Ensemble Sensitivity Fields that Diagnose Severe Convection**", B. Ancell and A. Coleman, 10th European Conference on Severe Storms, Krakow, Poland, Nov. 7, 2019.
25) "**The Nature and Variability of Ensemble Sensitivity Fields that Diagnose Severe Convection**", B. Ancell and A. Coleman, American Geophysical Union Annual Meeting, San Francisco, CA, Dec. 10, 2019.
26) "**Optimizing a Sensitivity-Based Ensemble Subsetting Technique for Convective-Scale Forecasts**", A.A. Coleman and B.C. Ancell, 30th Conference on Weather Analysis and Forecasting /26th Conference on Numerical Weather Prediction (American Meteorological Society Annual Meeting), Boston, MA, January 16, 2020.
27) "**Factors Influencing Ensemble Sensitivity-Based Targeted Observing Predictions at Convection-Allowing Resolutions**", A.J. Hill, C.C. Weiss, and B.C. Ancell, 24th Conference on Integrated Observing and Assimilation Systems for the Atmosphere, Oceans, and Land Surface (American Meteorological Society Annual Meeting), Boston, MA, January 15, 2020.
28) "**Using Ensemble Sensitivity Analysis to Identify Storm-Scale Characteristics Associated with Tornadic Potential in High-Resolution Idealized Supercells**", A.L. Hutson and C.C. Weiss, Severe Local Storms Symposium (American Meteorological Society Annual Meeting), Boston, MA, January 14, 2020.
29) "**Ensemble Subsetting for High-Impact Weather**", A.A. Coleman and B.C. Ancell, 4th

Convective Scale Modeling Workshop (National Center for Atmospheric Research), Boulder, CO, January 28, 2020.

30) "**Update: The Use of Ensemble Sensitivity to Improve Probabilistic Forecasts of High-Impact Events**", B.C. Ancell and A.A. Coleman, NWS SooConWest Meeting, El Paso, TX, February 10, 2020.

Graduate Student Involvement:

1) **Austin Coleman**, Ph.D. student - Development of ensemble sensitivity-based subsetting to improve probabilistic forecasts of severe convection.

2) Aaron Hill, Ph.D. student – Investigation of ensemble sensitivity-based observation targeting to improve forecasts of severe convection

3) **Jon Madden**, M.S. student – Integration of TTU forecast products into AWIPS2

4) **Abby Hutson**, Ph.D. student - Storm-scale ensemble sensitivity analysis to understand storm dependencies in the near-storm environment.

5) **Isaac Arseneau**, M.S. student – Assessment of sensitivity-based targeting for real data cases.

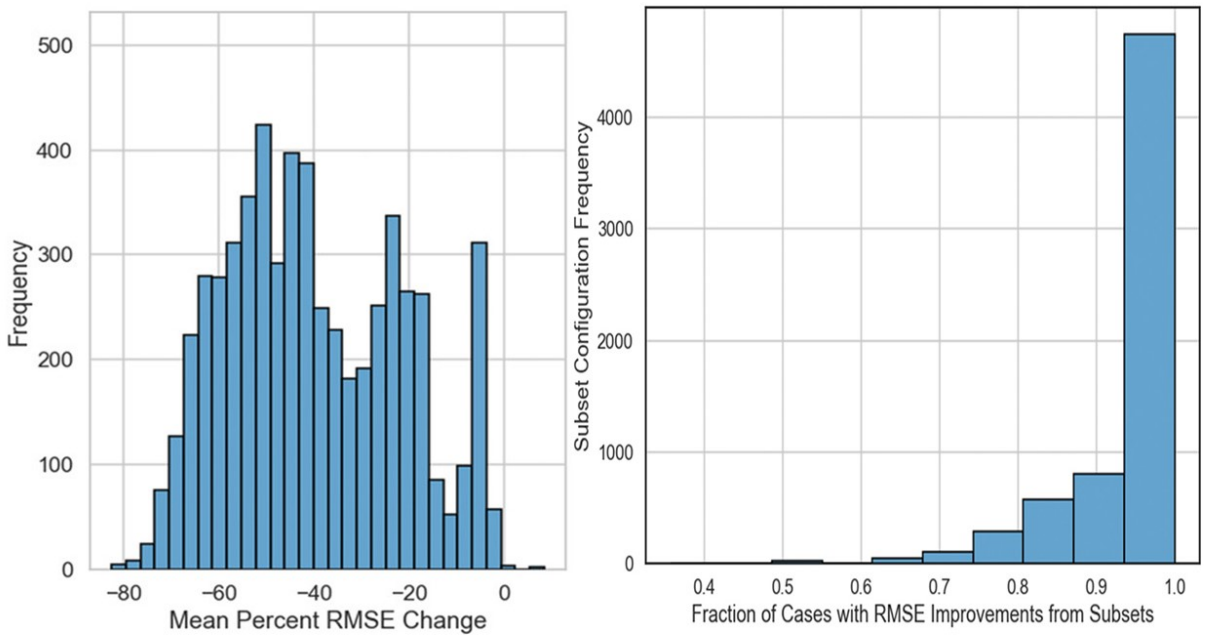

Figure 1 – Histograms depicting the frequency of levels of improvement (left panel) and the fraction of cases exhibiting improvements within the idealized ensemble sensitivity-based subsetting experiments.

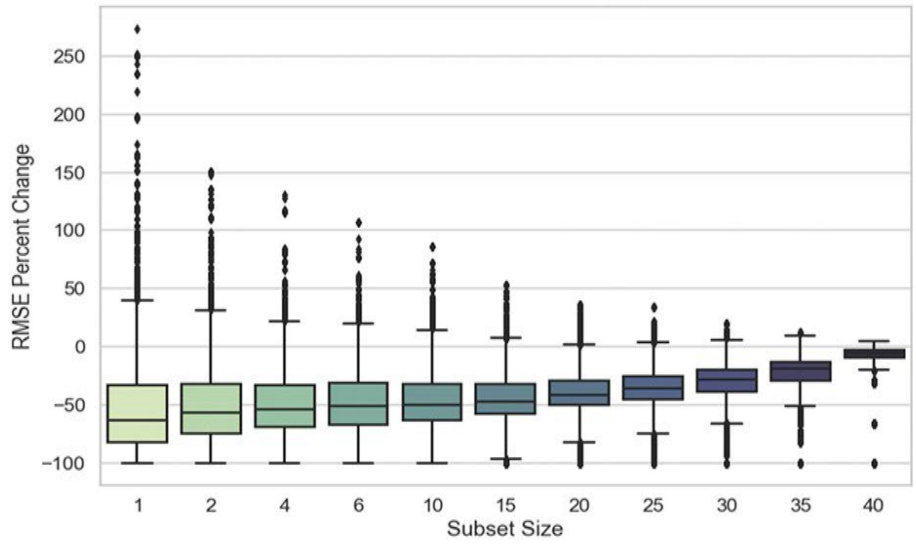

Figure 2 – The dependence of subset size on error reduction within the idealized ensemble sensitivity-based subsetting experiments.

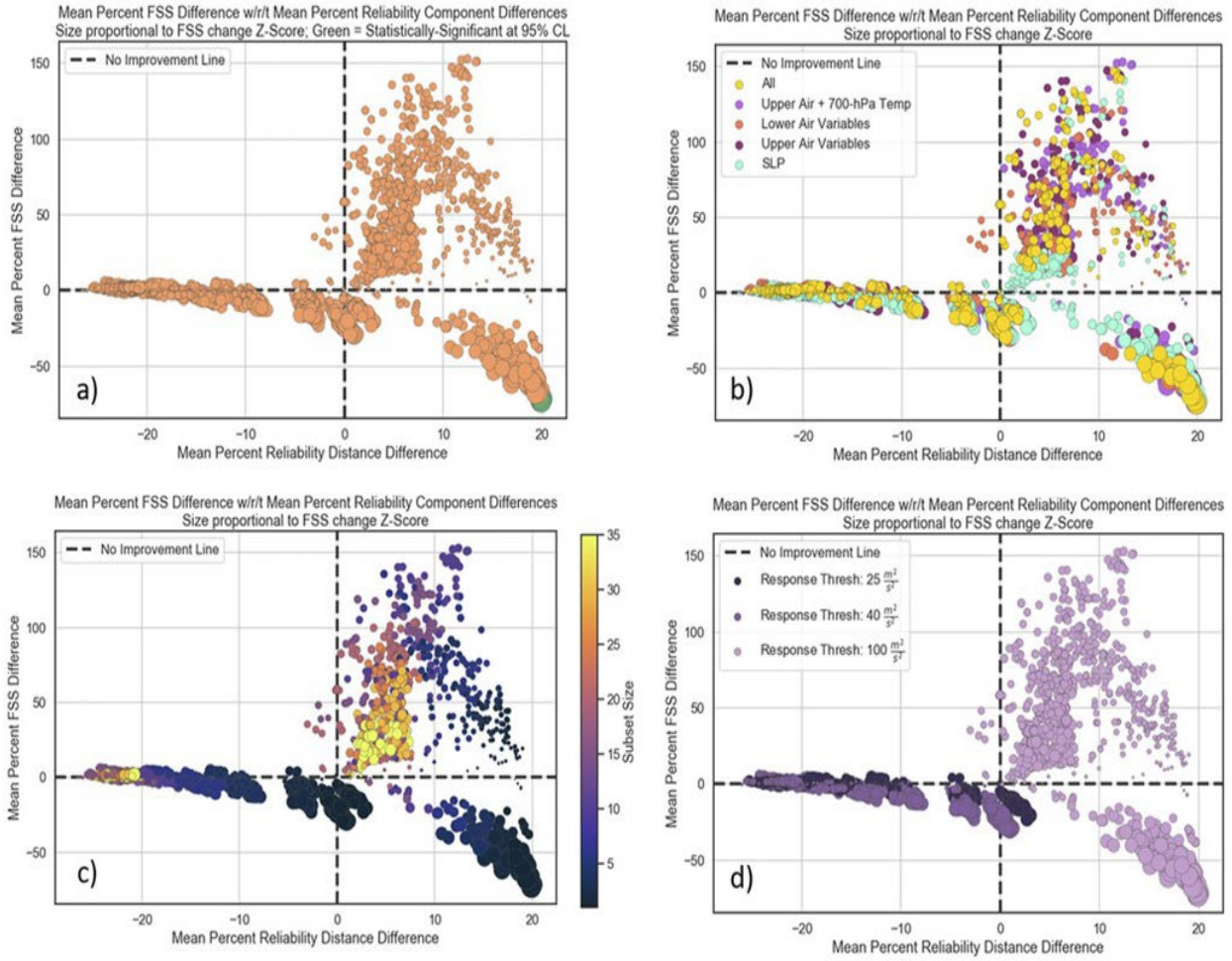

Figure 3 – Changes relative to the full ensemble for FSS and reliability for all configurations of the semi-idealized ensemble sensitivity-based subsetting experiments using updraft helicity as a response function.

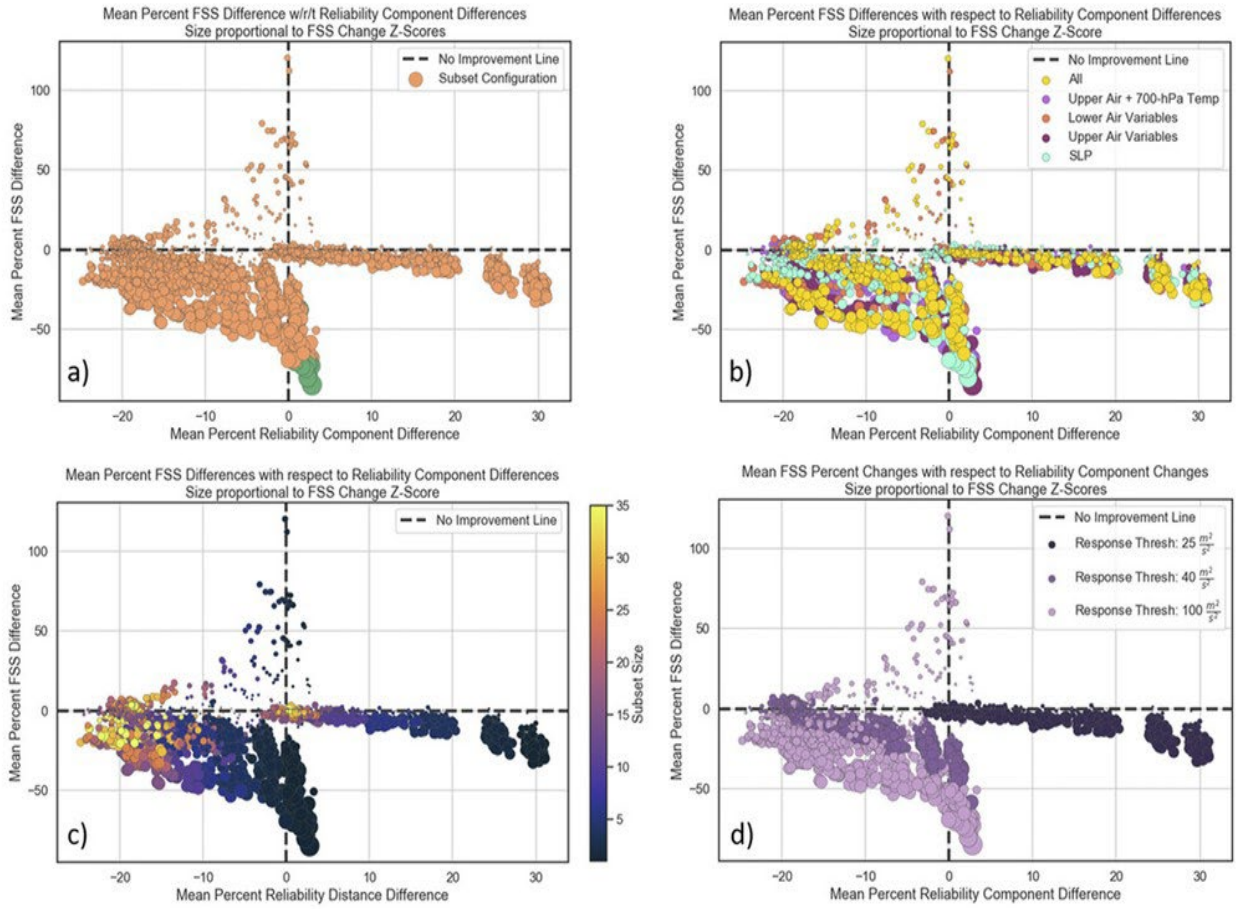

Figure 4 - Changes relative to the full ensemble for FSS and reliability for all configurations of the practical ensemble sensitivity-based subsetting experiments using updraft helicity as a response function.

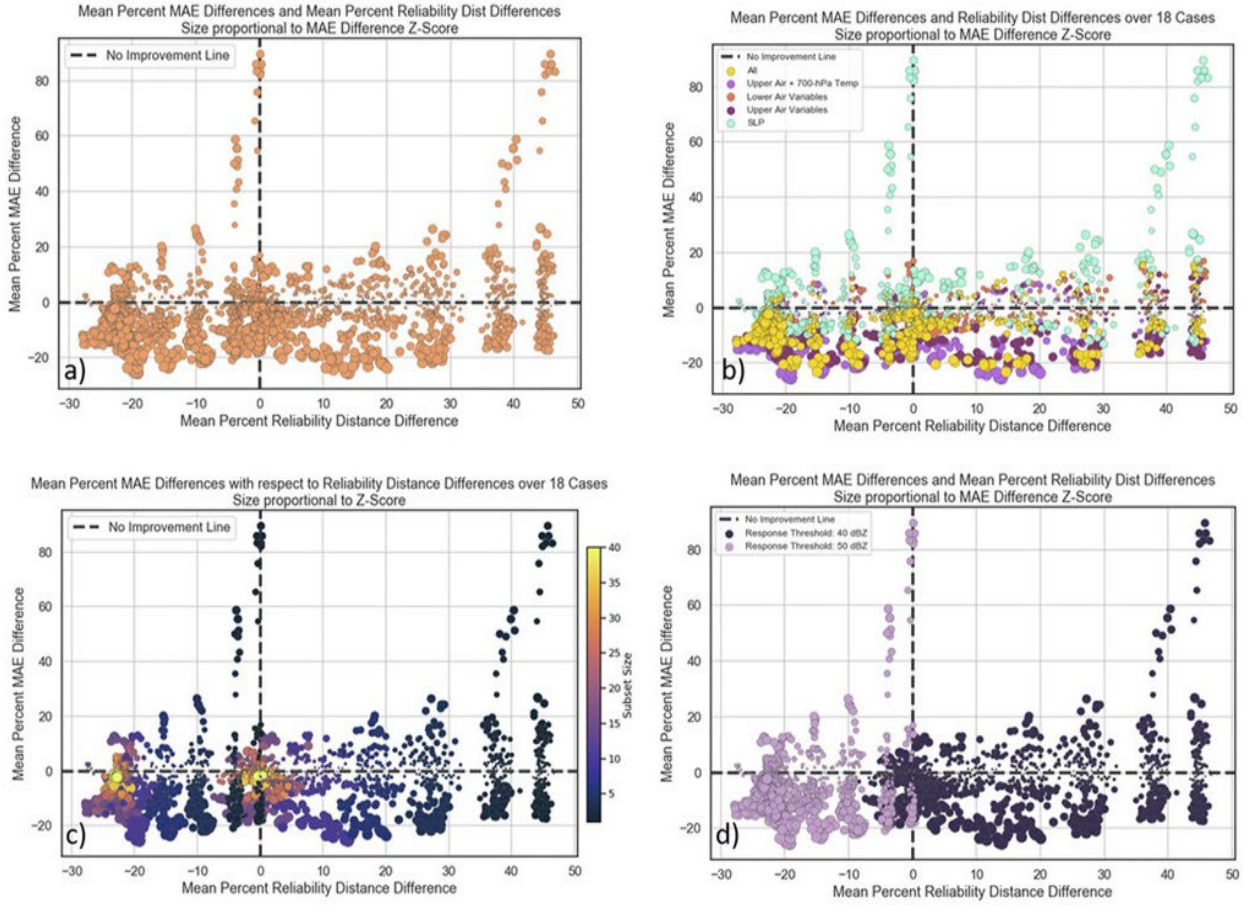

Figure 5 - Changes relative to the full ensemble for MAE and reliability for all configurations of the practical ensemble sensitivity-based subsetting experiments using simulated reflectivity as a response function.

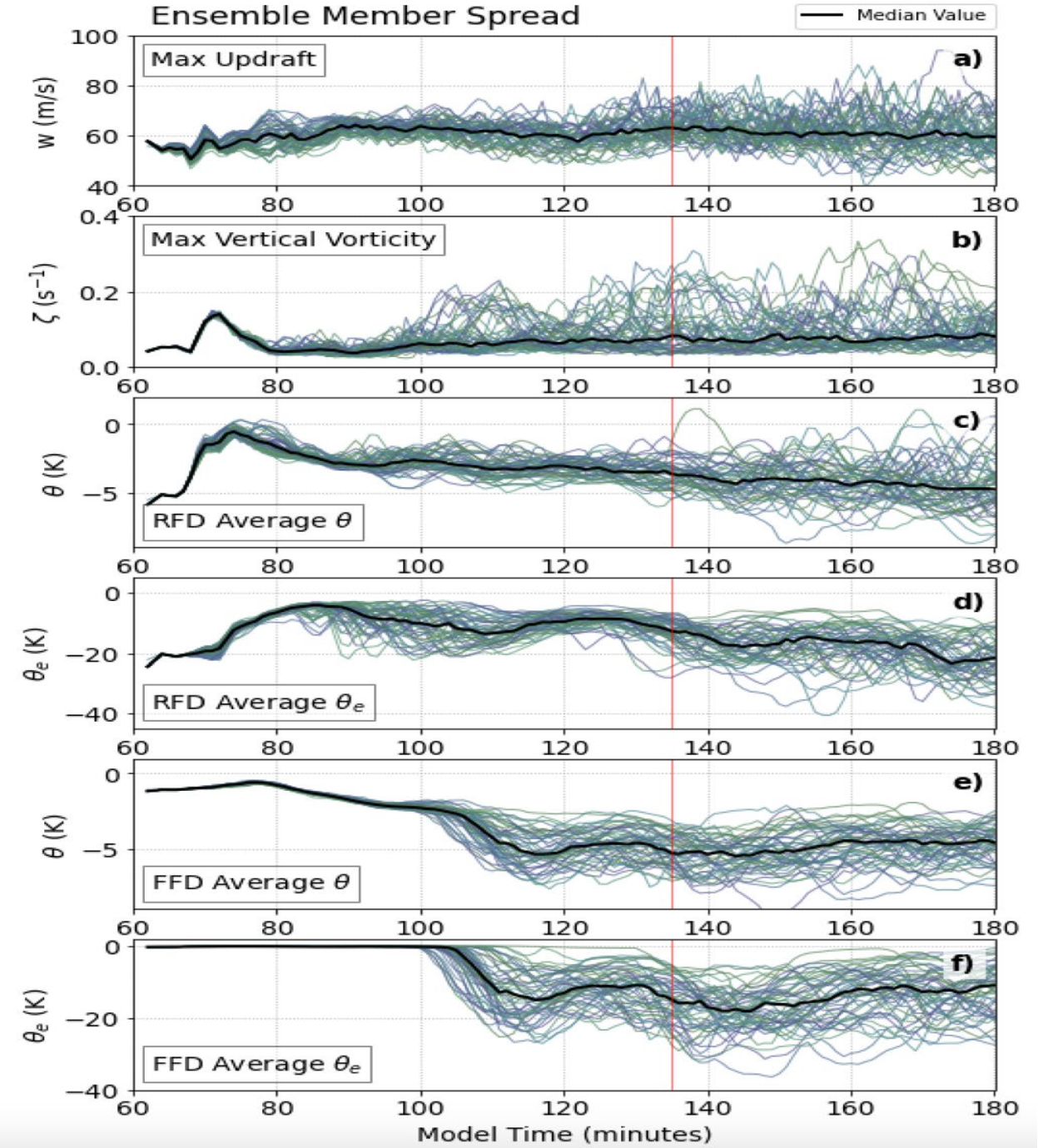

Figure 6 – Spaghetti plots showing the a) maximum vertical velocity, b) maximum vertical vorticity under the updraft, c) average potential temperature perturbation within the RFD, d) average equivalent potential temperature perturbation within the RFD, e) average potential temperature within the forward flank, and f) average equivalent potential temperature within the forward flank. All thermodynamic averages are taken withing a 2 km x 2 km box due southwest (northeast) of the mesocyclone for the RFD (FF). The bold black line indicates the median value for each metric.

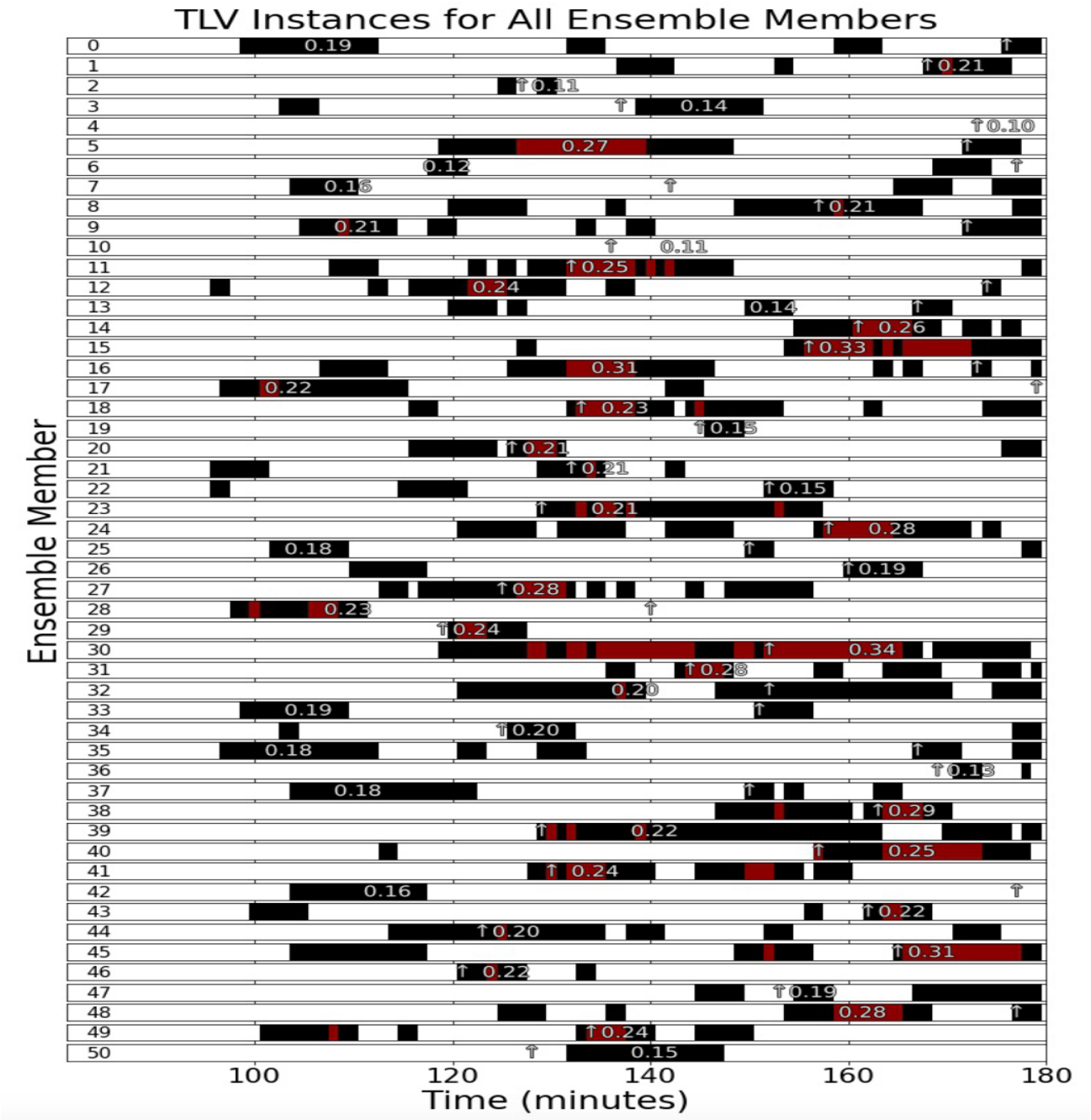

Figure 7 - A time series of TLV instances for each member in the ensemble, starting at t = 85 (20 minutes after perturbations were introduced). Each black bar indicates the occurrence of a TLV, and each red bar marks a TLV with vertical vorticity > 0.2 s^{-1}. There is one number for each ensemble member that is the magnitude of the strongest TLV over the lifetime of the member and is located at the time at which the maximum occurred. Each ensemble member is referenced by a number on the left side of each plot (the control member is number 0).

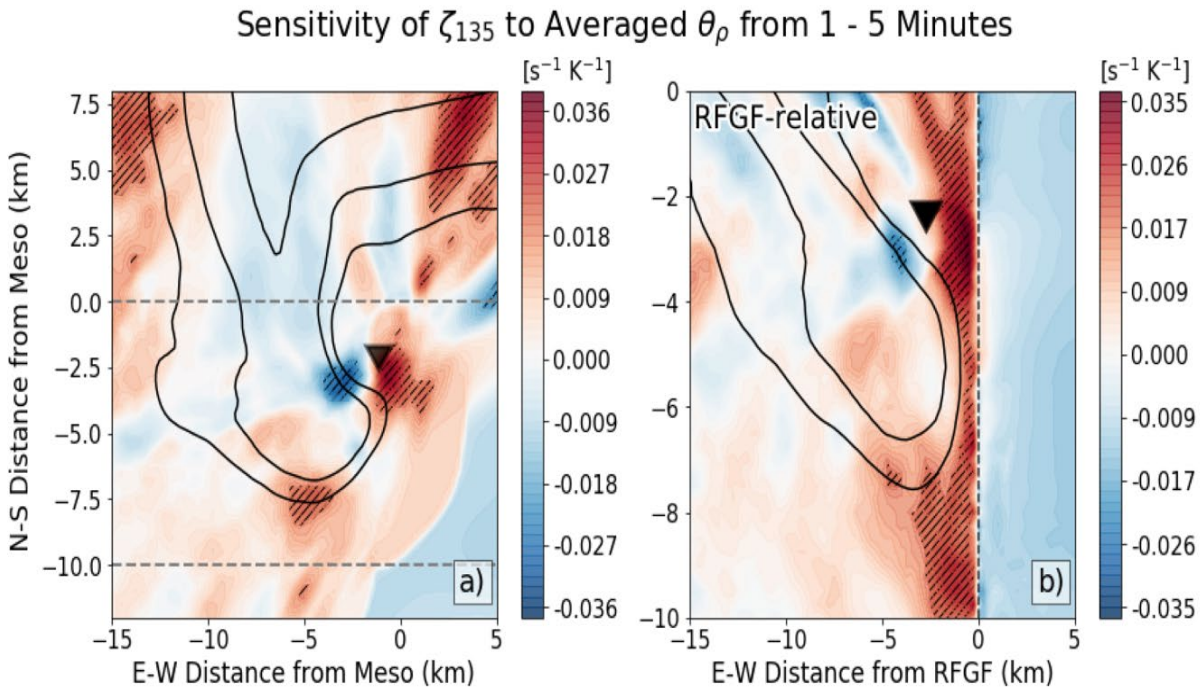

Figure 8 - A horizontal cross section of vertical vorticity sensitivity to (a) meso-relative and (b) RFGF-relative density potential temperature during the 5 min prior to TLV formation. Red color fill is positive sensitivity, and blue color fill is negative sensitivity. Areas with black hatching are areas of statistically significant sensitivity, using a one-sample t-test. Black solid contours indicate ensemble-averaged reflectivity (contoured at levels of 30, 40, and 50 dBZ). Gray horizontal dashed lines in (a) mark off the north-south extent of (b). The vertical black dashed line in (b) is the RFGF.

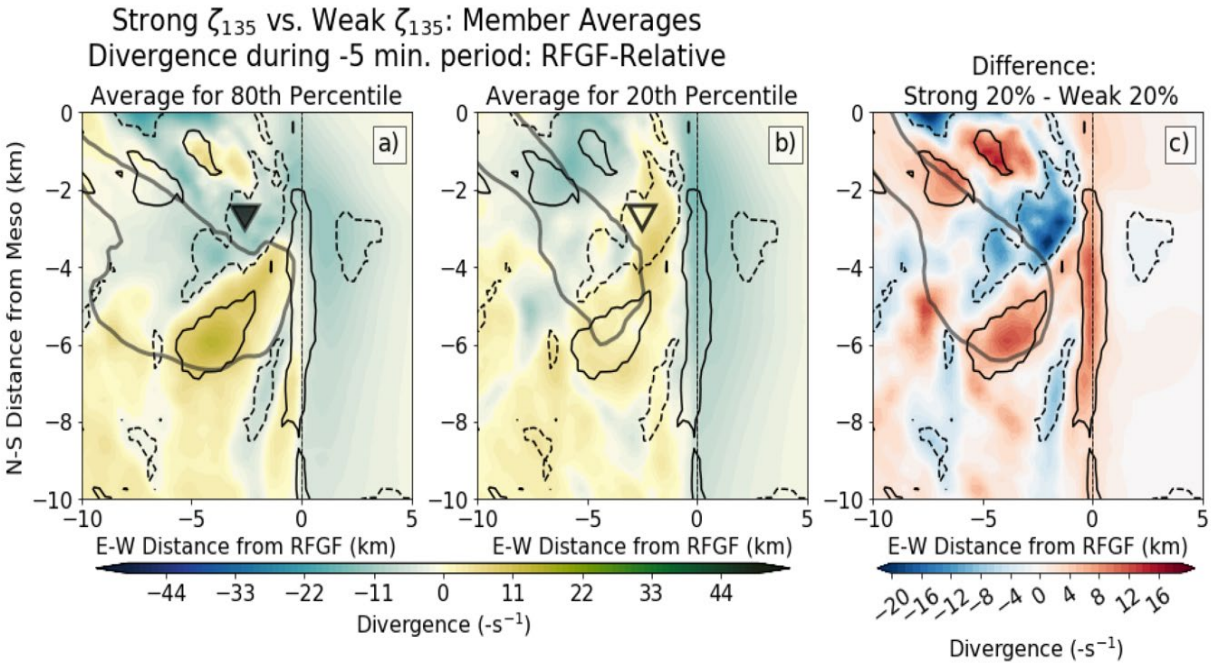

Figure 9 - Horizontal cross sections of RFGF-relative divergence averaged over member withvertical vorticity values within (a) the upper 80th percentile, (b) the lower 20th percentile, and (c)the difference between the two fields. Solid (dashed) black lines indicate regions of statistically significantly positive (negative) sensitivity of vertical vorticity to divergence. The thick grayline is the 40 dBZ radar reflectivity contour, and the vertical line at x = 0 indicates the location of the RFGF. The upside-down triangles mark the ensemble-averaged TLV location, with the filled triangle indicating that a TLV exists, and an outlined triangle indicating the expected location of the TLV if it were to form.

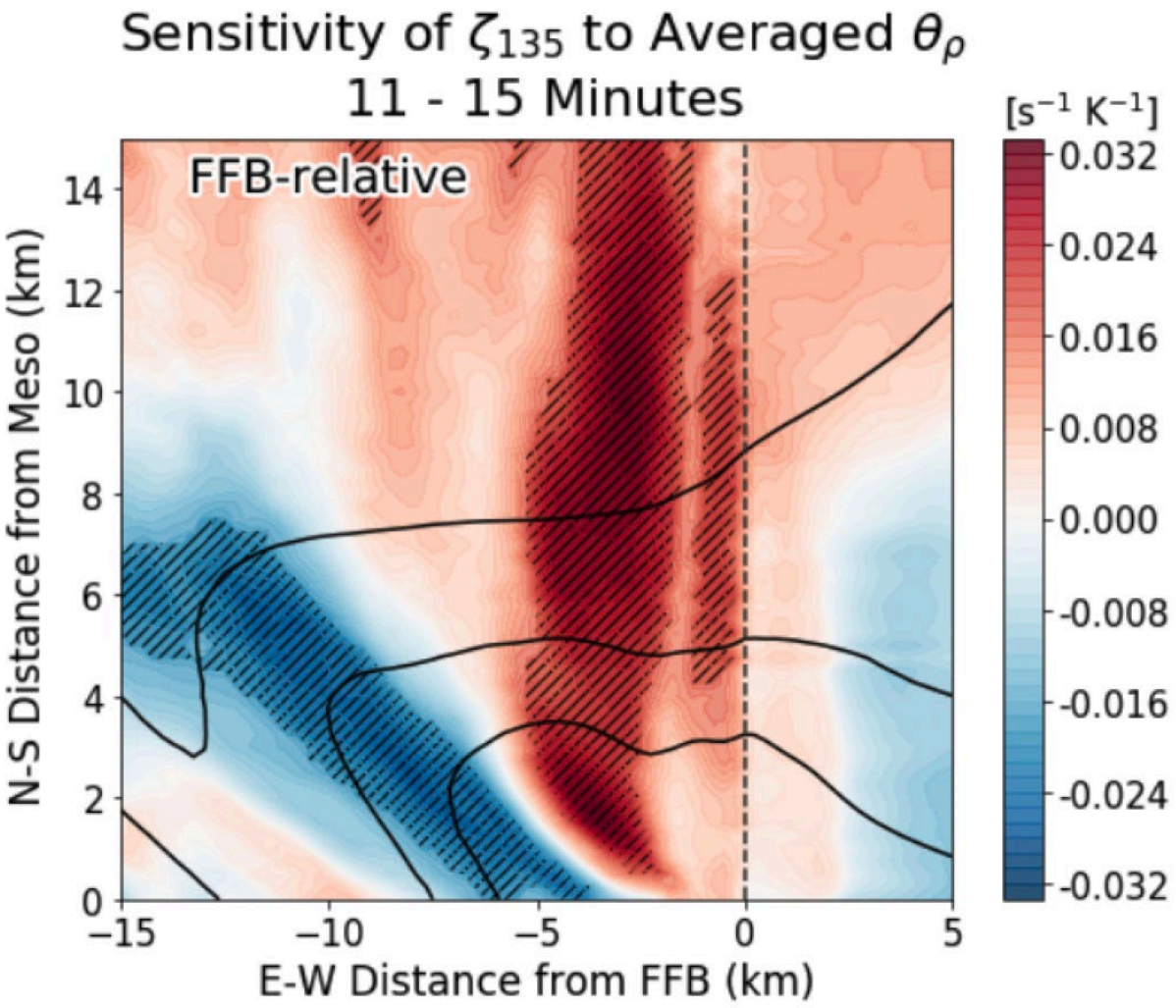

Figure 10 - Horizontal cross section of vertical vorticity sensitivity to FFB-relative density potential temperature during the 15-minute period prior to TLV formation. Lines and shading are as in Figure 8.

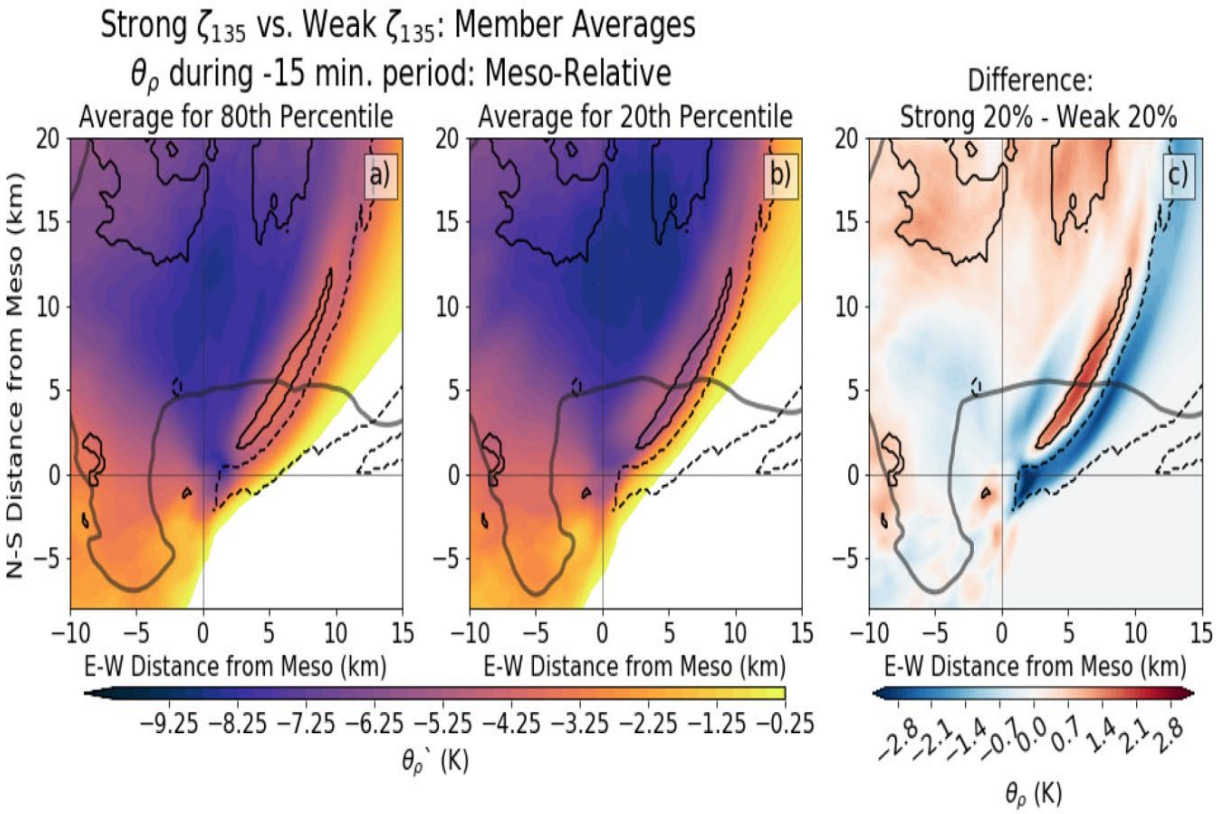

Figure 11 - Horizontal cross sections of perturbation density potential temperature during the 15-minute period prior to TLV formation, averaged over members with vertical vorticity values in the (a) upper 80th percentile, (b) lower 20th percentile, and (c) the difference between the two. Black solid (dashed) contours outline regions of positive (negative) sensitivity of vertical vorticity to density potential temperature, and the thick gray contour is the 40 dBZ radar reflectivity contour.

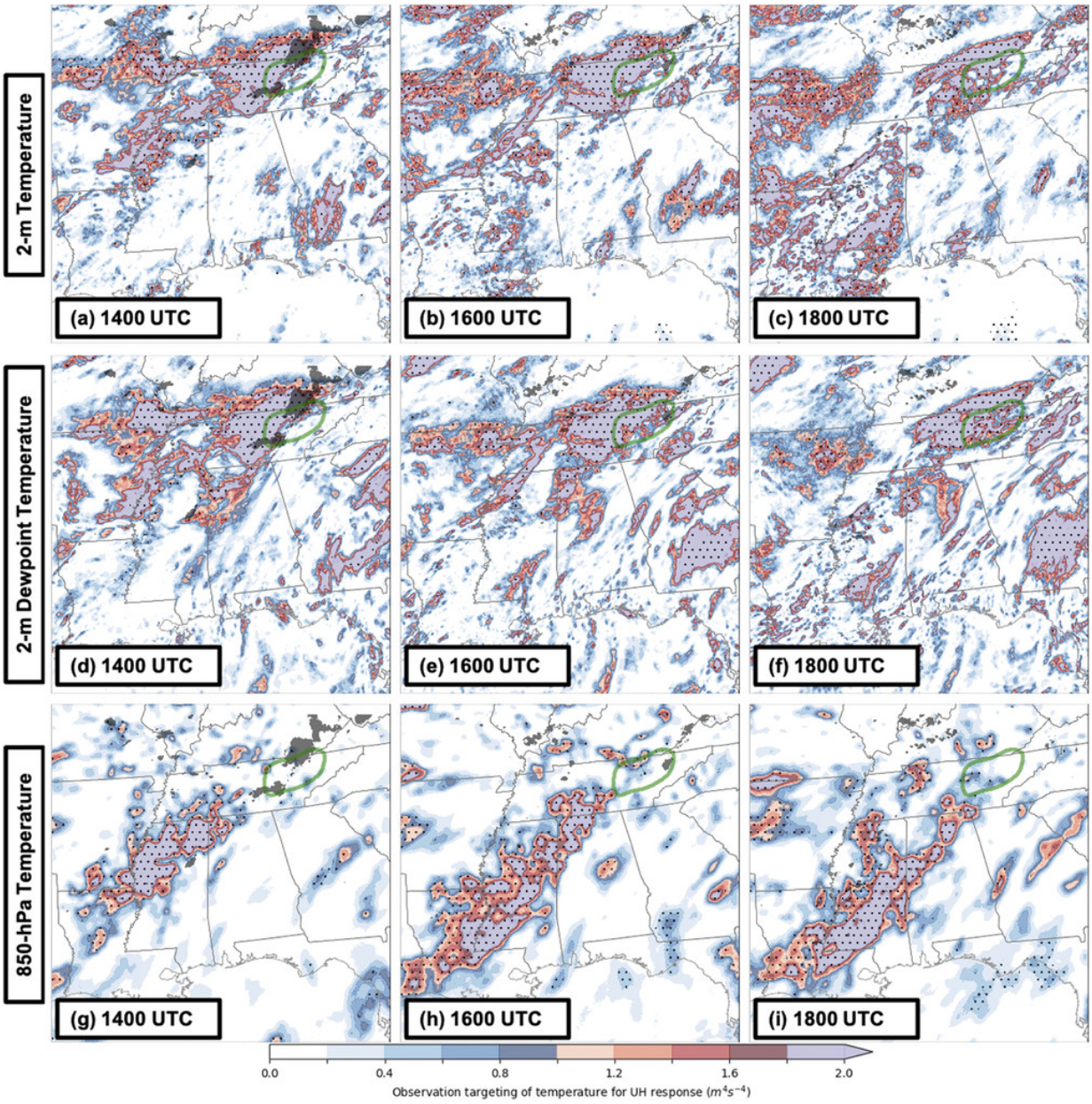

Figure 12 - Expected ensemble variance reduction (i.e., ESA targets) of UH response (m^4 s^{-4}; color shading) due to hypothetical assimilation of (a)–(c) 2-m temperature, (d)–(f) 2-m dewpoint temperature, and (g)–(i) 850-hPa temperature at (left) 1400; (center) 1600; and (right) 1800 UTC 22 Apr 2017 calculated from the 1200 UTC initialized CTRL ensemble forecast. Gray shading is the ensemble probability matched mean composite reflectivity greater than 40 dB*Z*. The green contour delineates the UH response region valid at 2200 UTC. Black dots denote geographical areas where the ensemble sensitivity passes a statistical significance test demonstrating the regression slope between initial condition and response variables is greater than zero with 95% confidence (Adapted from Hill et al. 2021).

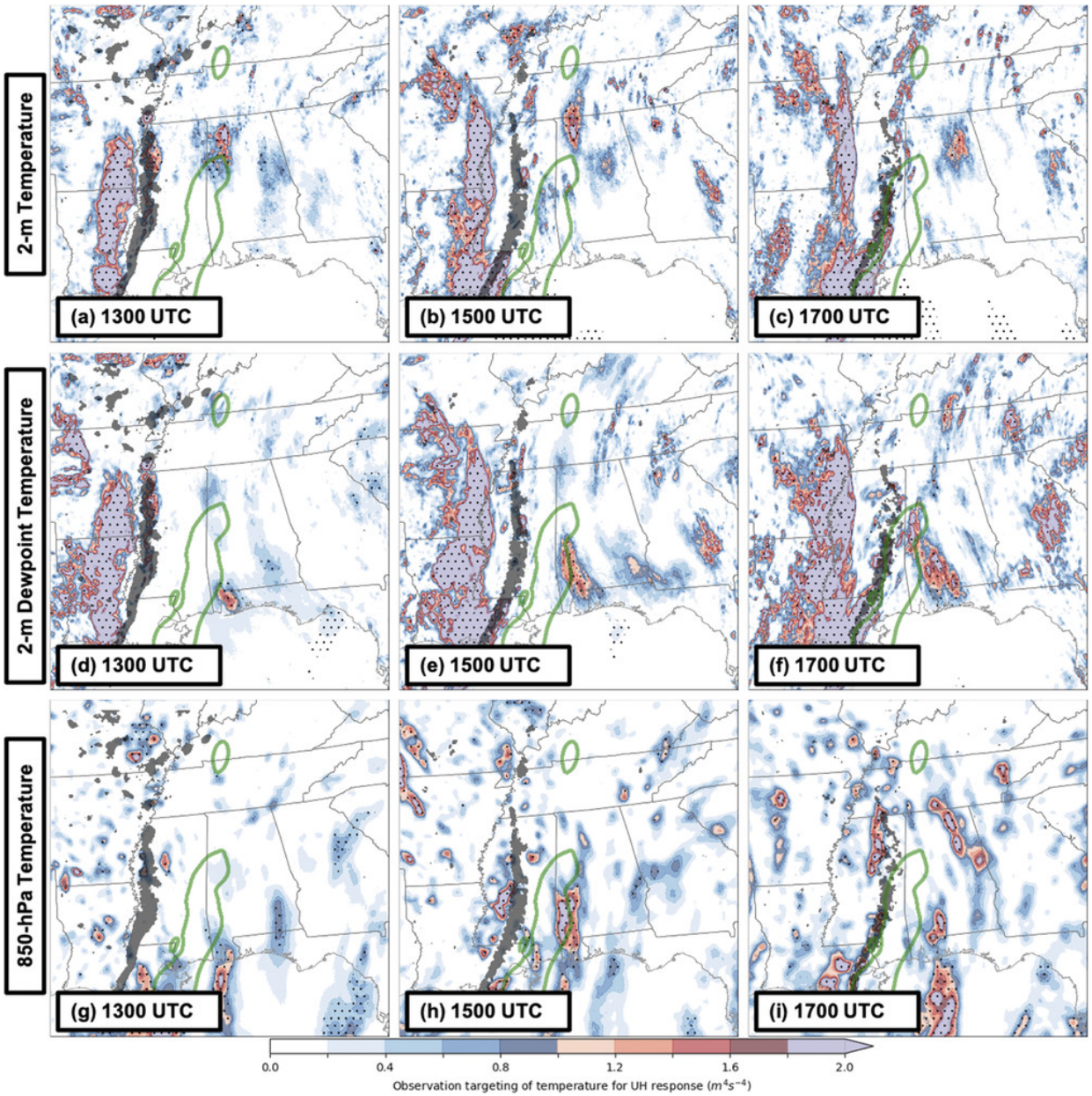

Figure 13 - As in Figure 12, but for the 30 Apr 2017 case. The response is valid at 1900 UTC and ESA-based targets are valid at (a),(c),(g) 1300; (b),(e),(h) 1500; and (c),(f),(i) 1700 UTC (Adapted from Hill et al. 2021).

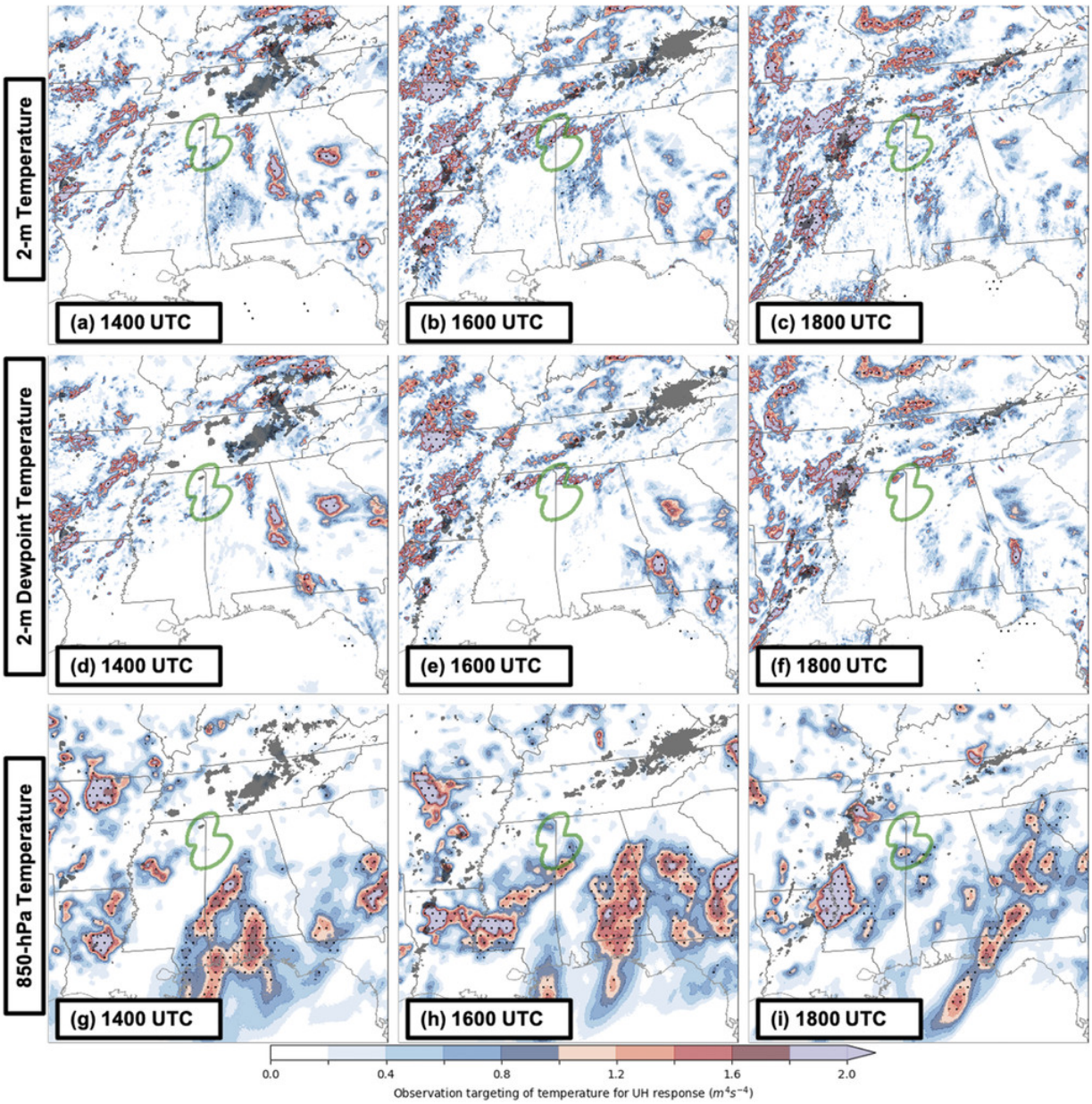

Figure 14 - As in Figure 12, but for the 23 Feb 2019 case. The response is valid at 0100 UTC 24 Feb 2019 and ESA-based targets are valid at (a),(c),(g) 1400; (b),(e),(h) 1600; and (c),(f),(i) 1800 UTC (Adapted from Hill et al. 2021).

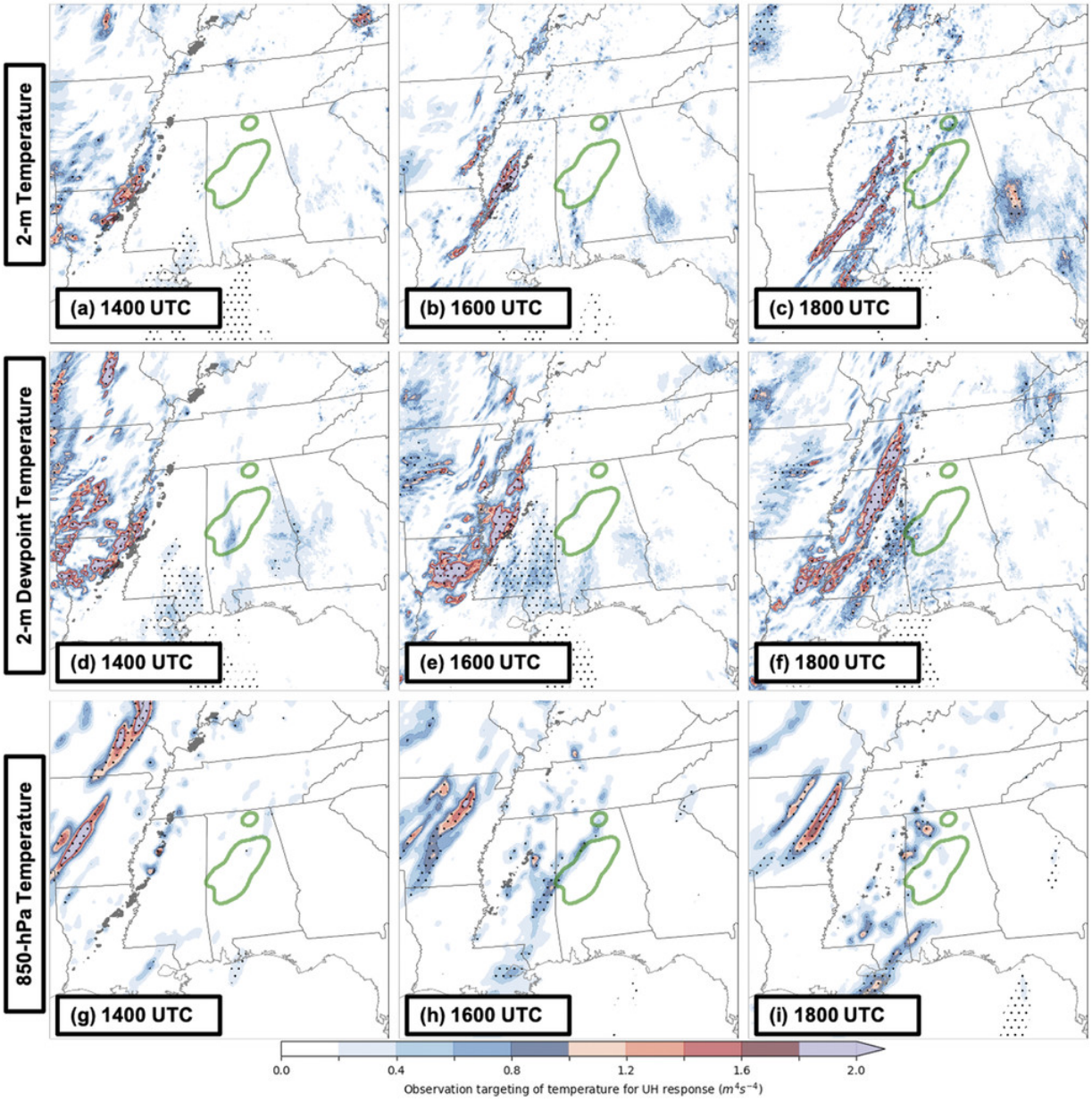

Figure 15 - As in Figure 12, but for the 14 Mar 2019 case. The response is valid at 2100 UTC and ESA-based targets are valid at (a),(c),(g) 1400; (b),(e),(h) 1600; and (c),(f),(i) 1800 UTC (Adapted from Hill et al. 2021).